

Modelling of standalone photovoltaic-wind-battery hybrid power systems using physics-based battery models

Mayur P. Bonkile

Department of Energy Science and Engineering,
Indian Institute of Technology Bombay,
Mumbai, India 400076
Email: bonkile.mayur@iitb.ac.in

Venkatasailanathan Ramadesigan*

Department of Energy Science and Engineering,
Indian Institute of Technology Bombay,
Mumbai, India 400076
Email: venkatr@iitb.ac.in

Abstract—Standalone hybrid power systems consist of one or more renewable energy sources (RES) along with battery energy storage (BES) system satisfying the power demand of the consumers. A generic framework is presented to evaluate the performance of a standalone PV-wind-BES hybrid power system using physics-based battery models. The system considered in this work comprises of PV panels, Maximum Power Point Tracking controller, wind turbine, power electronics, and lithium-ion batteries (LiBs). The dynamic behaviour of LiBs is simulated using a physics-based battery model. These models explicitly represent the transport and kinetic processes that take place within the LiB which help in understanding their operations and achieving better prediction of their performance. The framework for a standalone PV-wind-BES hybrid system is implemented in a MATLAB Simulink environment. A case study is provided using data from a remote residential area in India which includes variability in load demand and generation to demonstrate the effectiveness of the proposed framework. The physics-based battery models can be beneficial to analyse the thermal effect and capacity fade to make the best use of the BES in hybrid power systems.

Keywords: Standalone PV-wind-battery hybrid system; lithium-ion battery; physics-based battery models, P2D battery model

I. INTRODUCTION

A standalone hybrid power system is economical to install at remote locations, where power is produced and used without being transmitted to longer distances [1]. The power generated by renewable energy sources (RES) is used to meet the load demand, and the excess power is stored in the battery energy storage (BES) system. This stored power is used to provide electricity when the RES power is not enough or unavailable to satisfy the consumer load demand. Secondary lithium-ion batteries (LiBs) are becoming a technology of choice in off-grid BES applications due to its high energy and power density [2]. Generally, LiBs are modelled using equivalent circuit models that do not account for their internal states in simulation and control algorithms of hybrid power systems [3]. However, physics-based battery models offer better control and enable better utilisation of LiBs [4].

*Corresponding author

The main focus of this work is to illustrate how using physics-based battery models can save a significant amount of energy and cost with maximized safety, life, and usability. A schematic representation of the framework is shown in the figure 1. The power generated from RES is heavily

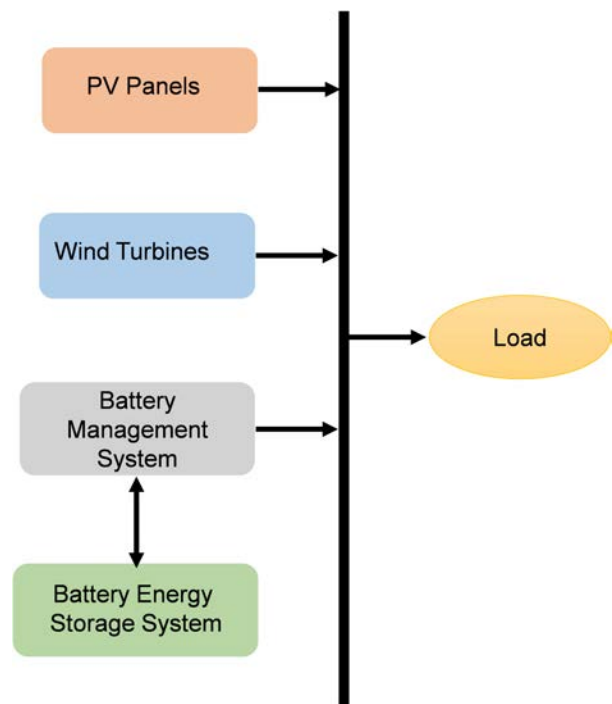


Fig. 1. Schematic of a proposed hybrid system

dependent on weather conditions and often times are an inadequate source of power. The standalone hybrid power system is an unreliable setup without being integrated with an energy storage system. The standalone hybrid power system coupled with an energy storage system can provide power in all weather conditions. The use of battery as an energy storage system is also an economically viable option [5].

There is a continuously increasing demand for long-lasting batteries with a higher power. A large share of the rechargeable batteries available today consists of LiBs. Lithium is a promising material in the battery production market because of its properties such as lightweight, high

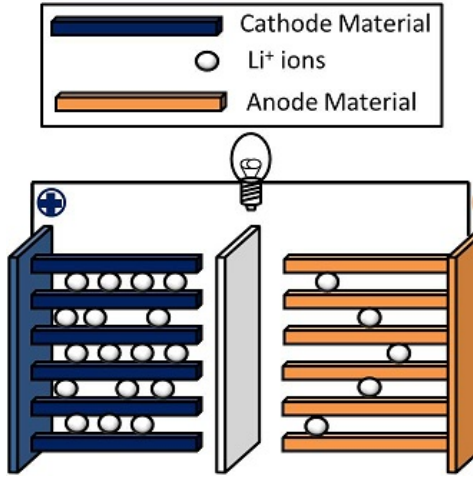


Fig. 2. Schematic representation of Li-ion battery [6]

electrochemical potential, etc. which help to achieve better power and energy density. A Li-ion battery is composed of several electrochemical cells connected in series and/or in parallel. Early batteries used lithium metal as a anode which has lot of safety issues. Today generally in LiBs, the anode and cathode are made from graphite and lithium metal oxide respectively, as shown in figure 2. A non-aqueous organic solvent with a lithium salt (LiPF_6) acts as the electrolyte. Electrical energy produced inside the battery is the result of redox reaction. At the anode oxidation reaction takes place to lose an electron and cation is formed. After this the electron flows through external circuit. The current collector is attached to anode and cathode, which guarantees the electrons to flow into the external circuit. Reduction reaction takes place at cathode by accepting the electron from the anode through the external circuit to form anion. Lithium ions which are formed at cathode insert into graphite after migrating across the electrolyte. A separator must be added if the electrolyte is liquid whereas the solid electrolyte acts as a separator. During charging and discharging, the lithium ions swing between anode and cathode as the reaction is reversible. LiBs face the problem of increased internal resistance, induce capacity loss, short life cycle which create complexity in understanding of the system. Merely depicting the system as a set of resistors and capacitors in series and parallel combination does not let us understand the actual physical phenomena occurring inside the battery. This work focusses on replacing a equivalent circuit based model for a LiB with a physics based model which enables to understand the underlying physics during the battery operation.

II. STANDALONE HYBRID POWER SYSTEM

The framework used in this study consists of PV panels, wind turbines, LiBs, and power electronics components. A single-diode equivalent circuit-based model is used to model the solar cells [7]. The equivalent circuit of the PV cell is shown in the figure 3. A differential algebraic equation based Maximum Power Point Tracking (MPPT) algorithm is implemented to track the maximum power point of the solar array [8, 9]. The major inputs for the proposed PV model are solar irradiation, PV panel temperature, and PV

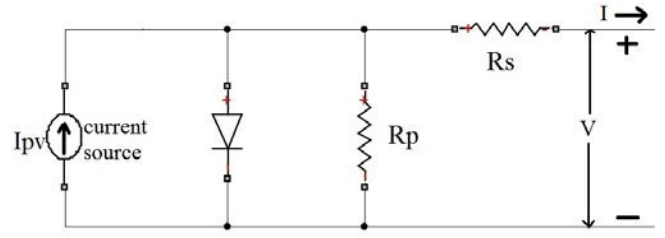


Fig. 3. Single-diode equivalent circuit-based model of a PV cell

manufacturing data sheet information, as given in the table I.

TABLE I
PARAMETERS FOR PV SYSTEM [10]

Parameter	Symbol	Value
Series resistance	R_s	0.221 Ω
Diode constant	a	1.3
Parallel resistance	R_p	415.405 Ω
Series-connected cells	N_s	54
Boltzmann constant	k	$1.3806503 \times 10^{-23}$ J/K
Electron charge	q	$1.60217646 \times 10^{-19}$ C
Current coefficient	K_I	0.0032 A/K
Nominal temperature	T_n	298.15 K
Nominal irradiation	G_n	1000 W/m ²
Nominal short-circuit voltage	$V_{oc,n}$	32.9 V
Nominal short-circuit current	$I_{sc,n}$	8.21 A
Voltage coefficient	K_v	-0.123 V/K
Light-generated current at the nominal condition	$I_{PV,n}$	8.214 A
Temperature	T	298.15 K

A DAE-based implementation of MPPT algorithm as given by Lee et al. [8] is implemented in the framework to operate the PV panels at MPPT as follows:

$$I(t) = I_{PV}(t) - I_o \left[\exp \left(\frac{V(t) + R_s I(t)}{V_{th} a} \right) - 1 \right] - \frac{V(t) + R_s I(t)}{R_p} \quad (1)$$

$$\frac{I(t)}{V(t)} = \frac{I_o \left(1 - R_s \frac{I(t)}{V(t)} \right) \exp \left(\frac{V(t) + R_s I(t)}{V_{th} a} \right)}{V_{th} a} + \frac{1 - R_s \frac{I(t)}{V(t)}}{R_p} \quad (2)$$

where $I(t)$ is the output current, $I_{PV}(t)$ is the PV current, I_o is the saturation current, and V_{th} is the thermal voltage. $V(t)$ is the output voltage, R_s is the series resistance, R_p is the parallel resistance, and a is the diode ideality constant. The following are the additional equations

$$V_{th} = \frac{N_s k T}{q} \quad (3)$$

$$I_{pv}(t) = [I_{pv,n} + K_I (T - T_n)] \frac{G(t)}{G_n} \quad (4)$$

$$I_o = \frac{I_{sc,n} + K_I (T - T_n)}{\exp \left(\frac{V_{oc,n} + K_v (T - T_n)}{a V_{th}} \right) - 1} \quad (5)$$

The power produced by the wind turbine varies as the cube of the wind speed and this power output from the wind turbine is predicted using wind speed and speed characteristics of the turbine, as shown in figure 4. The four characteristic parameters are cut-in wind speed (V_{ci}), rated

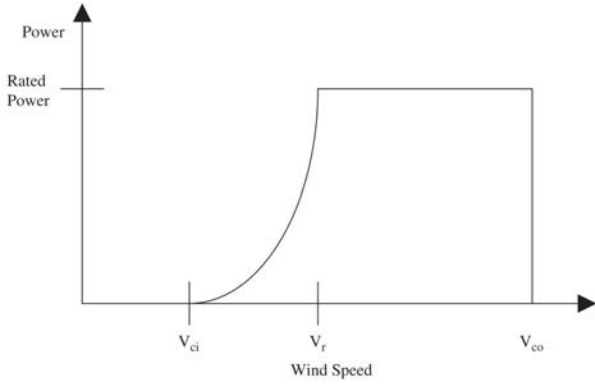


Fig. 4. Wind turbine characteristics

wind speed (V_r), cut-off wind speed (V_{co}) and rated power (P_{Rated}). The wind speed V_w at a turbine hub height H is calculated from the measured wind speed V_i at a reference height H_i . The value of power law index z depends on the topography and climatic condition, and in this work the value is taken as 0.2 [11].

$$\frac{V_w}{V_i} = \left(\frac{H}{H_i} \right)^z \quad (6)$$

The output power produced by the wind turbine is calculated as given by Deshmukh et al. [12]

$$P_{wind}(t) = \frac{1}{2} \rho A V_w(t)^3 C_p \eta_{inv} \eta_{mech} \quad (7)$$

$$P_{wind}(t) = \begin{cases} 0, & V_w(t) < V_{ci} \\ P_{wind}(t), & V_{ci} \leq V_w(t) \leq V_r \\ P_{Rated}, & V_r \leq V_w(t) \leq V_{co} \\ 0, & V_{co} < V_w(t) \end{cases} \quad (8)$$

where ρ represents the air density, A is swept area, C_p is the power coefficient and η_{inv} , η_{mech} represent inverter and mechanical components efficiency. The key parameters of the wind turbine used in the simulation are given in table II.

 TABLE II
PARAMETERS FOR WIND TURBINE [13]

Parameter	Symbol	Value
Swept area	A	15.9 m ²
Reference height	H_i	10 m
Turbine hub height	H	20 m
Rated power	P_{Rated}	5 kW
Cut-in wind speed	V_{ci}	1.5 m/s
Rated wind speed	V_r	10 m/s
Cut-off wind speed	V_{co}	52.5 m/s
Power law index	z	0.2
Mechanical components efficiency	η_{mech}	94 %
Inverter efficiency	η_{inv}	97 %
Number of blades		3

The use of physics-based LiB model instead of an equivalent circuit based model can help in better prediction of battery performance [4]. A detailed description of a finite volume method for a pseudo-two-dimensional (P2D) LiB

model [14] is given by Torchio et al. [15], which is used in this work for LiB simulation. This model includes diffusion in the electrolyte and solid phases, as well as Butler-Volmer kinetics. The P2D model consists of coupled and non-linear partial differential-algebraic equations in the cathode, separator and anode for the conservation of charge and mass. The detailed description of the P2D model formulation, its equations with boundary conditions and additional supporting equations, discretization and validation are explained elsewhere [15].

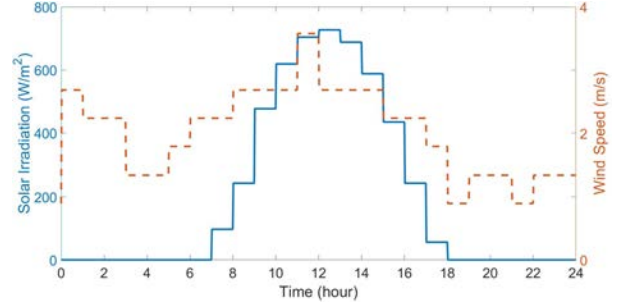


Fig. 5. Hourly average of solar irradiation and wind speed profile

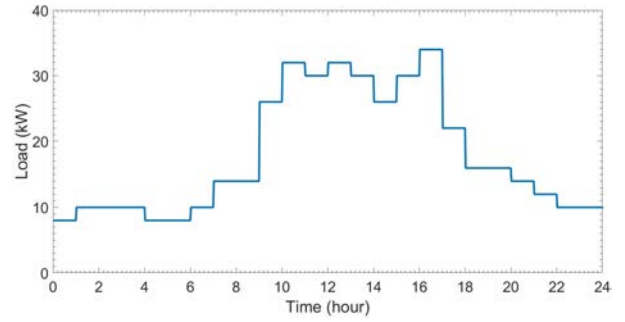


Fig. 6. Hourly load variations profile

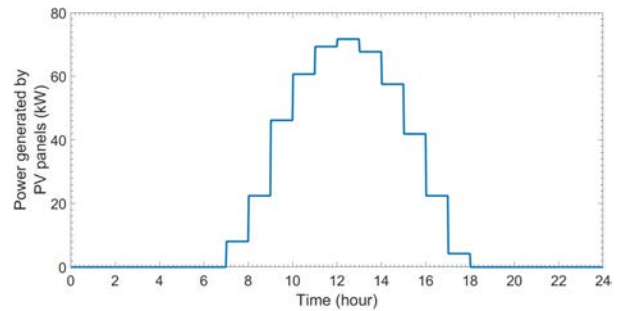


Fig. 7. Hourly power generated by PV panels

III. RESULTS AND DISCUSSION

The physics-based P2D model of LiBs integrated with the PV model, wind turbine model, MPPT controller, and other power electronics components were simulated simultaneously using real-world input data. All simulations were carried out on a system with Intel® Core™ i7-6700 CPU @3.40 GHz processor with 8 GB RAM. All simulations of the developed framework were performed in MATLAB® 2015a environment. The entire framework consisting of PV-wind-BES hybrid power plant were simulated simultaneously. The

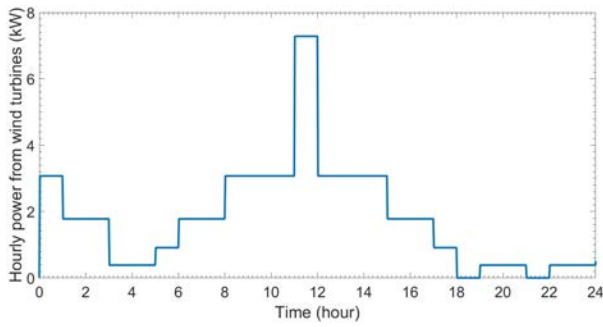


Fig. 8. Hourly power generated by wind turbines

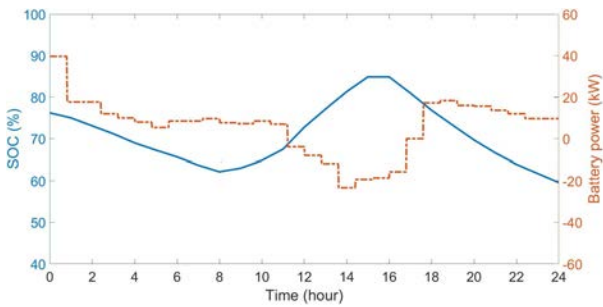


Fig. 9. Battery SOC and power

framework was simulated for a remote site at Wardha circle of Nagpur region (20.7453° N, 78.6022° E), located in India. The solar insolation profile is shown in figure 5 [16]. The actual wind data was collected for a selected site, as shown in figure 5 [17]. The purpose of using real-world input data enables us to study the behaviour of the proposed model under different operating conditions, weather, insolation and wind patterns. Figure 6 shows the hourly power demand obtained from MAHAVITARAN, Maharashtra State Electricity Distribution Co. Ltd. [18], which has to be satisfied by the hybrid power system. All the simulation results were obtained for 24 hour period. The PV power generated is shown in figure 7. Equations 1 to 5 were solved to calculate the maximum PV power generated. The PV power produced was high during high solar irradiation. The wind turbine behaviour is simulated for a given turbine with a rated power P_{Rated} , as shown in figure 8. The faster wind speed produces higher wind turbine power output. Figures 9 illustrates the hourly BES system power and state-of-charge (SOC) profile during the entire day. The positive value of battery power indicates the power supplied by it and a negative value means the power is stored during charging. The sun rises at 0600 hours, and the value of solar irradiance rises and falls until 1800 hours. The load profile is shown in figure 6. During the time intervals between midnight to 0600 hours and from 1800 to midnight, due to the absence of solar irradiation, the PV power generated is zero, as shown in figure 7. This shortfall was overcome by power supplied by both the BES system and wind turbines, as shown in figure 10. The total power predicted by the simulation results is found to be matching accurately with the load profile. From the figure 11, we can notice that from midnight to 0600 hours and 1800 to midnight, the battery SOC is decreasing. This was observed because the power generated by the RES

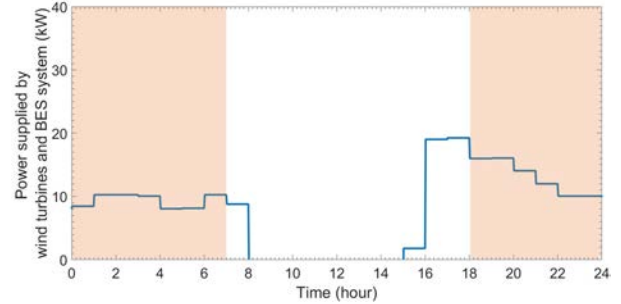
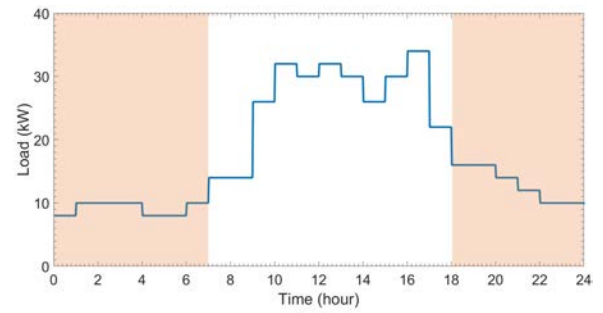


Fig. 10. Power supplied by wind turbines & BES during no sunshine hours

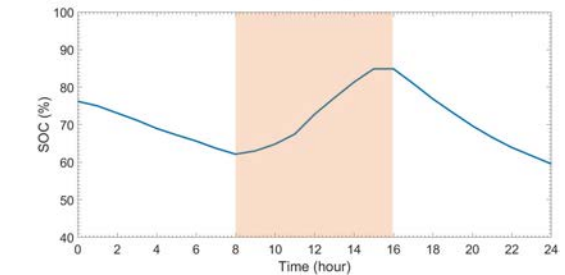
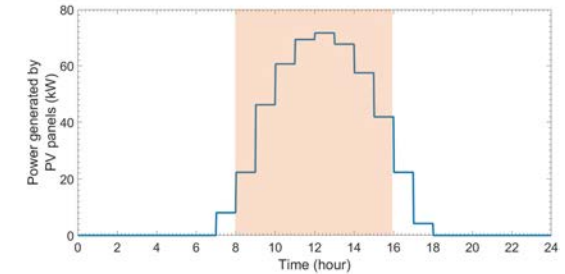
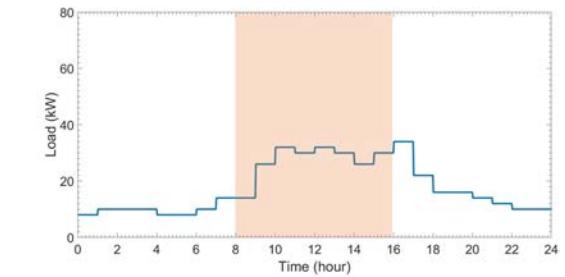


Fig. 11. Battery charging during sunshine hours

was less than the load demand, and the BES system has to meet the difference. Therefore, the battery was discharging during this time period, which results in lower SOC. During the sunshine period, the PV power produced was greater than the load demand. Therefore, the extra power generated over and above the load demand was used for the battery charging. Hence, increase in the battery SOC value was observed. These results demonstrate the performance of the

developed framework, which ensures the continuous power supply during day and night.

IV. CONCLUSION

In this paper, we have developed and demonstrated a framework to simulate the performance of PV-wind-BES hybrid power system in MATLAB Simulink environment. The BES system improves the reliability of the hybrid power system. The proposed framework of the hybrid power system includes a physics-based battery model representing the transport and kinetic processes inside the LiB instead of the typically used equivalent circuit based models. This framework would be helpful in optimal sizing of the storage systems that prevent under-utilization and over-stacking of batteries. This framework is generic in nature and can be easily extended further to include a combination of several RESs and different storage technologies for hybrid power systems. However, hybrid power system performance prediction done through this framework has some limitations because of the inherent uncertainty of solar insolation and wind pattern has a strong effect on simulation results. In the future, the developed framework would be extended further to incorporate resource uncertainties.

REFERENCES

- [1] D. Nelson, M. Nehrir, and C. Wang, "Unit sizing and cost analysis of stand-alone hybrid wind/pv/fuel cell power generation systems," *Renewable Energy*, vol. 31, no. 10, pp. 1641 – 1656, 2006.
- [2] V. Ramadesigan, P. W. C. Northrop, S. De, S. Sathnanagopalan, R. D. Braatz, and V. R. Subramanian, "Modeling and simulation of lithium-ion batteries from a systems engineering perspective," *Journal of The Electrochemical Society*, vol. 159, no. 3, pp. R31–R45, 2012.
- [3] E. M. Natsheh and A. Albarbar, "Solar power plant performance evaluation: simulation and experimental validation," *Journal of Physics: Conference Series*, vol. 364, no. 1, p. 012122, 2012.
- [4] V. Ramadesigan, "Electrochemical-engineering-based models for lithium-ion batteries—past, present, and future," *The Electrochemical Society Interface*, vol. 26, no. 2, pp. 69–71, 2017.
- [5] A. Pena-Bello, M. Burer, M. K. Patel, and D. Parra, "Optimizing PV and grid charging in combined applications to improve the profitability of residential batteries," *Journal of Energy Storage*, vol. 13, pp. 58 – 72, 2017.
- [6] "Schematic representation of li-ion battery." https://commons.wikimedia.org/wiki/File:Schematic_of_a_Li-ion_battery.jpg. Accessed: 2019-01-31.
- [7] J. C. H. Phang, D. S. H. Chan, and J. R. Phillips, "Accurate analytical method for the extraction of solar cell model parameters," *Electronics Letters*, vol. 20, no. 10, pp. 406–408, 1984.
- [8] S. B. Lee, C. Pathak, V. Ramadesigan, W. Gao, and V. R. Subramanian, "Direct, efficient, and real-time simulation of physics-based battery models for stand-alone pv-battery microgrids," *Journal of The Electrochemical Society*, vol. 164, no. 11, pp. E3026–E3034, 2017.
- [9] M. P. Bonkile and V. Ramadesigan, "Power management control strategy using physics-based battery models in standalone pv-battery hybrid systems," *Journal of Energy Storage*, vol. 23, pp. 258 – 268, 2019.
- [10] "Parameters of the Kyocera KC200GT solar array." <https://www.kyocerasolar.com/dealers/product-center/archives/spec-sheets/KC200GT.pdf>. Accessed: 2019-01-31.
- [11] G. Notton, M. Muselli, P. Poggi, and A. Louche, "Decentralized wind energy systems providing small electrical loads in remote areas," *Int. J. Energy Res.*, vol. 25, pp. 141–164, 2001.
- [12] M. Deshmukh and S. Deshmukh, "Modeling of hybrid renewable energy systems," *Renewable and Sustainable Energy Reviews*, vol. 12, no. 1, pp. 235 – 249, 2008.
- [13] "Parameters of the Aeolos-V 5kW wind turbine." <https://en.wind-turbine-models.com/turbines/1853-aeolos-aeolos-v-5kw>. Accessed: 2019-01-31.
- [14] M. Doyle, T. F. Fuller, and J. Newman, "Modeling of galvanostatic charge and discharge of the lithium/polymer/insertion cell," *Journal of The Electrochemical Society*, vol. 140, no. 6, pp. 1526–1533, 1993.
- [15] M. Torchio, L. Magni, R. B. Gopaluni, R. D. Braatz, and D. M. Raimondo, "Lionsimba: A matlab framework based on a finite volume model suitable for li-ion battery design, simulation, and control," *Journal of The Electrochemical Society*, vol. 163, no. 7, pp. A1192–A1205, 2016.
- [16] "Photovoltaic Geographical Information System - Interactive Maps." <http://re.jrc.ec.europa.eu/pvgis/apps4/pvest.php>. Accessed: 2019-01-31.
- [17] "Weather report for nagpur region india." https://www.wunderground.com/history/airport/VANP/2011/1/5/DailyHistory.html?req_city=&req_state=&req_statename=&reqdb.zip=&reqdb.magic=&reqdb.wmo. Accessed: 2019-01-31.
- [18] "Hourly feeder load information: Maharashtra State Electricity Distribution Co. Ltd." <http://www.mahadiscom.co.in/feeder-hourly-data/hourly-feeder-load-information.shtm>. Accessed: 2019-01-31.